Potential of Withaferin-A, Withanone and Caffeic Acid Phenethyl ester as ATP-competitive inhibitors of BRAF: A bioinformatics study

Vidhi Malik [a], Vipul Kumar [a], Sunil C. Kaul [b], Renu Wadhwa [b,**], Durai Sundar [a,*]

[a] DAILAB, Department of Biochemical Engineering & Biotechnology, Indian Institute of Technology (IIT)-Delhi, Hauz Khas, New Delhi, 110-016, India
[b] AIST-INDIA DAILAB, DBT-AIST International Center for Translational & Environmental Research (DAICENTER), National Institute of Advanced Industrial Science & Technology (AIST), Tsukuba, 305-8565, Japan

ARTICLE INFO

ABSTRACT

Serine/threonine-protein kinase B-raf (BRAF) plays a significant role in regulating cell division and proliferation through MAPK/ERK pathway. The constitutive expression of wild-type BRAF (BRAF^{WT}) and its mutant forms, especially V600E (BRAF^{V600E}), has been linked to multiple cancers. Various synthetic drugs have been approved and are in clinical trials, but most of them are reported to become ineffective within a short duration. Therefore, combinational therapy involving multiple drugs are often recruited for cancer treatment. However, they lead to toxicity and adverse side effects. In this computational study, we have investigated three natural compounds, namely Withaferin-A (Wi-A), Withanone (Wi-N) and Caffeic Acid Phenethyl ester (CAPE) for anti-BRAF^{WT} and anti-BRAF^{V600E} activity. We found that these compounds could bind stably at ATP-binding site in both BRAF^{WT} and BRAF^{V600E} proteins. In-depth analysis revealed that these compounds maintained the active conformation of wild-type BRAF protein by inducing αC-helix-In, DFG-In, extended activation segment and well-aligned R-spine residues similar to already known drugs Vemurafenib (VEM), BGB283 and Ponatinib. In terms of binding energy, among the natural compounds, CAPE showed better affinity towards both wild-type and V600E mutant proteins than the other two compounds. These data suggested that CAPE, Wi-A and Wi-N have potential to block constitutive autophosphorylation of BRAF and hence warrant *in vitro* and *in vivo* experimental validation.

1. Introduction

The discovery of the class of human tumors dependent on mutant BRAF kinase has paved the way for the design and development of RAF inhibitors as potential therapeutic drugs (Holderfield et al., 2014). The RAF kinase family - ARAF, BRAF and CRAF kinases are the essential components of the ERK signaling pathway. This pathway also known as the RAS–RAF–MEK–ERK signaling pathway, plays an important role in regulating cell growth and differentiation by mediating signals between the cell surface receptors and the nucleus (Avruch et al., 2001). Similar to other kinases, RAF consists of the N terminal lobe and C terminal lobe connected with a short flexible hinge. The ATP binding site, DFG motif and activation loop are present at the interface of these lobes. The activation of RAF required a closed conformation of the lobes with unfolded activation segment, DFG motif and αC-helix in the inward position (Figs. 1C and 2). When activated, RAF kinases cause phosphorylation and

activation of MEK1 and MEK2 kinases. Phosphorylated MEK1 and MEK2 kinases subsequently activate ERK1 and ERK2. Activated ERK, phosphorylates numerous substrates both in the cytosol and the nucleus, which stimulate proliferation and survival of the cells (Karoulia et al., 2017; Haling et al., 2014). The commonly observed dysregulation of the ERK signaling in cancer cells is the result of mutations occurring in different components of this pathway. Among human cancers, approximately 8% involve BRAF mutations in which Val at position 600 (in the activation segment of this kinase) is changed most frequently to Glu (Karoulia et al., 2017). This substitution causes hyperactivation of kinase activity by many folds (Grasso et al., 2016). Other common substitutions found in the activation loop include V600K, V600D and V600R (Ascierto et al., 2012). Because of these mutations present in the kinase domain, efforts to target the ERK signaling pathway by developing ATP competitive inhibitors have increased. In the absence of upstream activity, RAF assumes an inactive conformation (monomeric and closed) in normal

Fig. 1. (A) Structure of compounds selected for the study. (B) Structure of BRAF-MEK1 dimer (PDB ID: 4MNE) selected for the study. (C) Structure of BRAF^{WT}-BGB283 dimer complex. The structural elements around ATP/ligand-binding site of protein are highlighted that includes activation loop (shown in firebrick red color), αC-helix (orange) and P loop (salmon). (For interpretation of the references to color in this figure legend, the reader is referred to the Web version of this article.)

cells. The activation of RAF is regulated by the small GTPases consti-tuting the RAS family proteins (KRAS, NRAS and HRAS). The inactive RAS-GDP proteins are converted to active RAS-GTP form in the plasma membrane when upstream receptors are activated by growth factors. The RAF-RAS-GTP complex is formed due to the translocation of RAF to the membrane when the levels of RAS-GTP increase. This fully activates RAF by processes involving priming, homodimerization and heterodimeriza-tion involving the kinase domain (Karoulia et al., 2017; Haling et al., 2014).

RAF inhibitors, on the other hand, have a less complex mechanism of action. In general, the RAF kinase inhibitors are broadly classified on the basis of their mechanism of stabilization of the target. One of the most common challenges in drug discovery and development for BRAF inhi-bition is BRAF dimerization. In view of this, the efforts are focused on modifying ATP-competitive inhibitors in order to prevent negative allo-steric binding, leading to paradoxical activation (Haling et al., 2014). Different processes that lead to RAF activation should also be considered while designing these inhibitors. Vemurafenib (VEM) and BGB283 are ATP competitive inhibitors of BRAF with different mechanisms of action. BGB283 favors the active conformation of BRAF protein (αC-helix-In) and enrich RAF-MEK1 complexes. On the other hand, VEM favors inac-tive conformation of BRAF (αC-helix-out), thereby inhibit the kinase activity of BRAF and weakens MEK1 binding (Karoulia et al., 2017). VEM was the first drug developed against the most common mutant of BRAF, i.e., V600E (BRAF^{V600E}), which blocks ATP binding in DFG-In and αC-helix-Out conformation for melanoma patients (Croce et al., 2019). However, VEM can activate the MAPK pathway by inducing BRAF-CRAF dimerization. This activation leads to various skin related side effects. It has also been reported that 10–20% of patients treated with BRAF in-hibitors develop squamous cell carcinoma (Munoz-Couselo et al., 2015). Although it showed promising results initially, it was later found that patients treated with BRAF inhibitors get resistant within a year (Sanchez et al., 2018). The novel RAF inhibitor BGB283 serves as a dual inhibitor for both RAF and EGFR. Previously reported pre-clinical studies have

shown that BGB283 had a better response against BRAF and its mutants than first generation inhibitors such as VEM (Tang et al., 2015). The BGB283 was established to be within the acceptable risk profile and response in BRAF mutated melanoma, thyroid and endometrial cancers. Various clinical studies are going on to investigate the safety and efficacy of BGB283 alone and in combination with other inhibitors (Desai et al., 2020). Other than these drugs, Dabrafenib and Encorafenib are the BRAF kinase inhibitors that have been approved against BRAF mutants related melanoma (Proietti et al., 2020; Savoia et al., 2019). Dabrafenib, which was approved by FDA in 2013, is known to selectively bind and inhibit the activity of the BRAF (Ballantyne and Garnock-Jones, 2013). It has been found to be effective against BRAF V600E, V600D, V600R and V600K mutant cell lines (Gentilcore et al., 2013; King et al., 2013). Further, Encorafenib, approved in 2018, is a selective ATP competitive RAF kinase inhibitor (Shirley, 2018). It is used in combination with binimetinib in adults with metastatic melanoma with BRAFV600 muta-tions (Shirley, 2018; Delord et al., 2017).

The major limitation in cancer therapeutics is the development of drug resistance in cancer cells within a few months of treatment. Therefore, multiple synthetic drugs are used for the treatment of all cancers, which results in multiple adverse side-effects in the patients, Hence the adjuvant treatment with natural compounds is preferred (Newman and Cragg, 2016). Numerous natural products and/or their derivatives in the past have been approved against multiple cancers, which have been reported in detail elsewhere (Huang et al., 2021; Newman and Cragg, 2020). Specific to BRAF inhibition, natural com-pounds such as dehydrosilybins, Piperlongumine, Rocaglamides, and others have been documented to be effective in recent pre-clinical studies (Fofaria et al., 2017; Diukendjieva et al., 2020). In this study, we have investigated the potential of three natural molecules, namely, Withaferin-A (Wi-A), Withanone (Wi-N) from Ashwagandha (*Withania sominifera*) and Caffeic acid phenethyl ester (CAPE) from honeybee propolis against wild type BRAF (BRAF^{WT}) and BRAF^{V600E} mutant using computational simulations. The ADME/toxicity prediction as well as
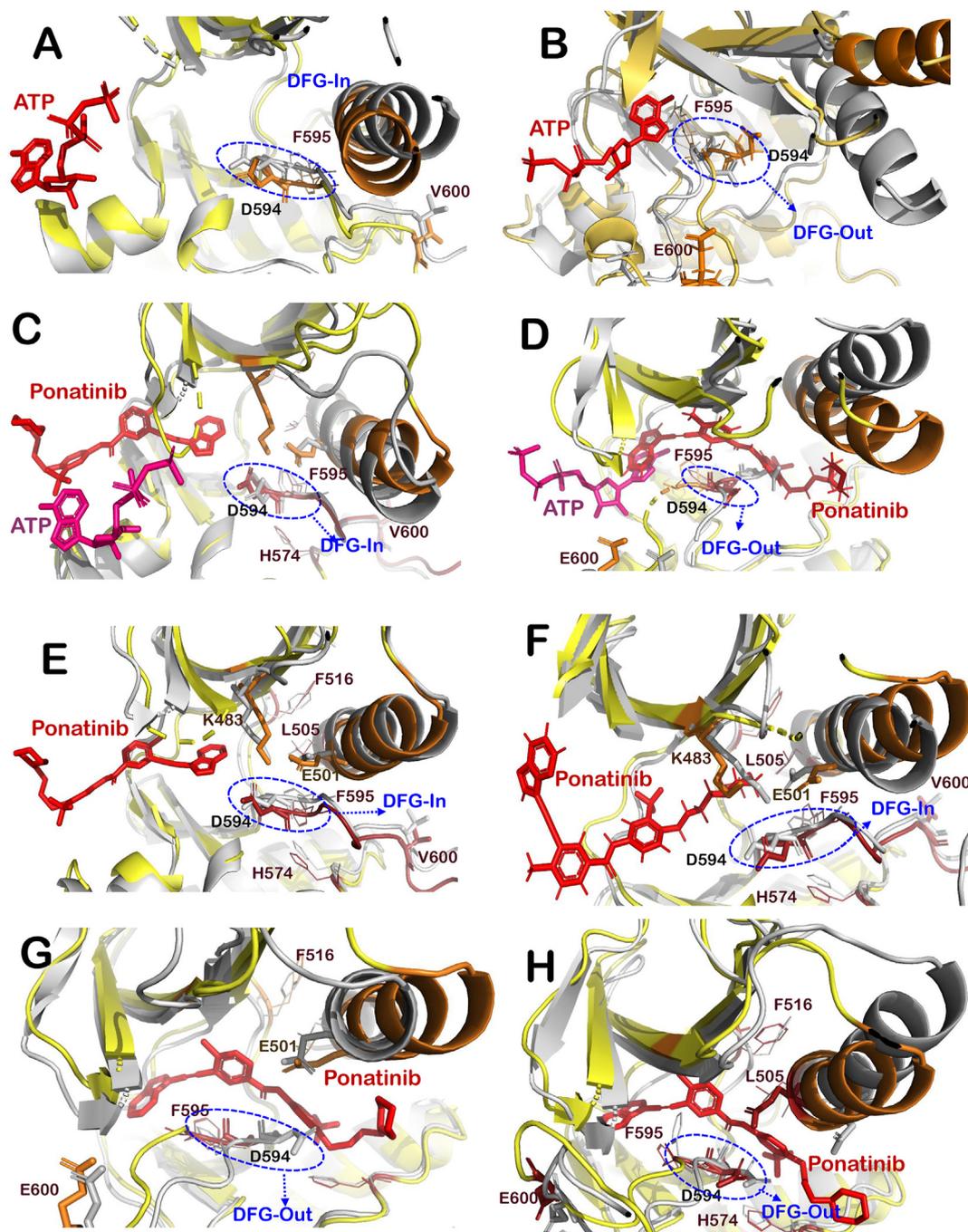
Fig. 2. The changes in the structure of the BRAF^WT and BRAF^V600E with and without ligands. (A) Superimposition of active BRAF^WT apo protein (grey) with BRAF^WT -ATP complex (yellow-red). (B) Superimposition of BRAF^V600E apo protein structure (grey) with that of BRAF^V600E-ATP complex (yellow-red). (C) Superimposition of active BRAF^WT -ATP complex (grey) with BRAF^WT -Ponatinib complex (yellow-red). (D) Superimposition of BRAF^V600E -ATP complex (grey) with that of BRAF^V600E-Ponatinib complex (yellow-red). (E) Superimposition of BRAF^WT protein structure (grey) with that of BRAF^WT-Ponatinib complex (yellow-red) at chain B. (F) Superimposition of BRAF^WT protein structure (grey) with that of BRAF^WT-Ponatinib complex (yellow-red) at chain C. (G) Superimposition of BRAF^V600E protein structure (grey) with that of BRAF^V600E-Ponatinib complex (yellow-red) at chain B. (H) Superimposition of BRAF^V600E protein structure (grey) with that of BRAF^V600E-Ponatinib complex (yellow-red) at chain C. (For interpretation of the references to color in this figure legend, the reader is referred to the Web version of this article.)

non-toxic doses of these compounds have already been reported earlier (Nishikawa et al., 2015; Yadav et al., 2017). The previous studies showed that these compounds follow the Lipinski rule of five for oral bioavailability, with moderate toxicity (Nishikawa et al., 2015; Yadav et al., 2017). They are moderately soluble in water and have lipophilic characteristics. Gastrointestinal absorption was high for all the compounds, while Wi-A and Wi-N were predicted to be non-permeant for the blood brain barrier (Nishikawa et al., 2015; Yadav et al., 2017). These compounds have been reported to possess multimodal anticancer activity

(Ozturk et al., 2012; Widodo et al., 2010; Yu et al., 2017). In various studies, these compounds have been shown to possess anticancer activities involving various molecular mechanisms such as by disruption of p53-Mortalin interaction, downregulation of PARP1, inhibition of nuclear translocation of NFkB etc. (Ichikawa et al., 2006; Sari et al., 2020). Such mechanisms of anticancer activities have yet not been fully described and evidenced. Given the previous reports on the mechanism of anticancer activities of various drugs and the similarity of structures in kinases, we performed structure-based inverse virtual screening at the

ATP binding site of several kinases (Malik, 2020). The results showed EGFR, ABL and BRAF were among the top hits and indicated that these compounds could serve as a dual inhibitor of EGFR and BRAF like BGB283. In a recently published study, we reported that these molecules might serve as ATP competitive inhibitors against various EGFR mutants, including exon 20 insertion mutations of EGFR (Malik et al., 2021).

Further, a combination of Wi-A and Sorafenib has been shown to have a synergistic effect against papillary and anaplastic cancer cell lines via caspase-3 and PARP (Poly (ADP-ribose) polymerase cleavage, down-regulation of BRAF and inhibition of heat shock proteins (Cohen et al., 2012). Additionally, the combination of CAPE and electroporation has been found to be effective against wild type and V600E mutant melanoma cell lines (Choromanska et al., 2020). In spite of the existing evidence that these natural molecules could inhibit the BRAF-related activation of cancer cell proliferation, none of the studies have shown their binding kinetics against wild type and mutant BRAF proteins. Hence, in this study, *in silico* investigation of the binding potential, dynamics and crucial interactions of these three molecules (Wi-A, Wi-N and CAPE) at the ATP-binding site of BRAF^{WT} and BRAF^{V600E} has been carried out using BGB283, Ponatinib and VEM as positive controls (Fig. 1A).

2. Computational methods

2.1. Preparation of the structures

The potential of CAPE, Wi-A and Wi-N to serve as ATP competitive inhibitors of BRAF^{WT} and BRAF^{V600E} mutant activity was explored in this study. The method used here is similar to our previously published study (Malik et al., 2021). Crystal structure of active conformation of BRAF^{WT} (extracted from BRAF-MEK1 dimer (PDB ID: 4MNE)) and BRAF^{V600E} (PDB ID: 6P7G) were obtained from Protein Data Bank (Fig. 1B and C) (Haling et al., 2014; Wan et al., 2004). Protein and ligands structures were prepared using Schrodinger 2018-4 modules, PrepWizard and LigPrep, respectively (Protein Preparation Wizar, 2018). The protein preparation was done using protein preparation wizard in three steps - (i) addition of missing hydrogens, removal of water, and filling of missing loops and side chains (ii) systems were analyzed and irrelevant heteroatoms used for crystallization were removed and finally (iii) H-bond assignment at pH 7.0 was done and structure was minimized using OPLS3e forcefield. The Protein preparation was followed by ligand preparation, which was done using the LigPrep module of Schrodinger. Ligand preparation steps included the generation of possible ionization sates at pH 7.0 ± 2, desalting and generating tautomers and stereoisomers at most 32 per ligand.

2.2. Molecular docking

The ATP-binding site of BRAF was targeted to check the inhibitory effects of test compounds (Wi-A, Wi-N and CAPE) by molecular docking followed by MD simulations of docked complexes. BGB283, VEM and Ponatinib are already known ATP competitive inhibitors of BRAF protein and therefore, they were used as the control in our study. The glide extra precision (XP) algorithm was used to perform docking of ligands at the ATP binding site of protein (Protein Preparation Wizar, 2018; Friesner et al., 2006). Firstly, the grid of 10 Å^3 was generated at the ATP binding site using the Glide Grid module, further, the ligand docking was done with Glide extra precision algorithm keeping all the parameters at default.

2.3. Molecular dynamics simulations in explicit water model

The docked complexes were simulated to monitor the stability of the ligand-bound complexes and conformational changes induced by them using the Desmond module of the Schrodinger suite (Protein Preparation Wizar, 2018). The protein-ligand complexes were simulated in the OPLS3e force field in a TIP4P solvated periodic box with 10 Å spacing.

The solvation of the complexes was followed by neutralization, minimization for up to 2000 iterations. Minimized system was heated up to 300 K, equilibrated and simulated for a time period of 100 ns. The protocol and algorithms used for minimization and simulations are described elsewhere (Kumar et al., 2021). All the simulations carried out in this study were performed under identical conditions using exactly same parameters, including custom initial seed value (2007) for velocity randomization. RMSD, hydrogen bonds analysis and conformational changes over the simulation trajectories of protein-ligand complexes were monitored using VMD version 1.9.4 (Humphrey et al., 1996). The MM/GBSA free binding energy was calculated by selecting the average structure from the stable trajectory using uniform weighting and then crucial interactions throughout the simulations were calculated using the Prime module of Schrodinger suite. The protein-protein binding energy in the presence and absence of control and test compounds were calculated using PRODIGY webserver (Vangone and Bonvin, 2015; Xue et al., 2016).

3. Results

The potential of natural compounds to serve as ATP competitive inhibitors of BRAF^{WT} and BRAF^{V600E} mutant protein was explored. Ponatinib, BGB283 and VEM were taken as the positive control. Ponatinib is an FDA approved drug for the treatment of chronic myeloid leukemia, it is a multitargeted receptor tyrosine kinase inhibitor, which could target BRAF, VEGFR, FEGFR and Bcr-abl (Cotto-Rios et al., 2020; Tan et al., 2019; Muller et al., 2017) VEM is an FDA-approved type-I inhibitor for BRAF^{V600E} mutant melanoma that acts by inducing αC-helix-Out and DFG-In conformation of BRAF. On the other hand, BGB283 is a type-II dual inhibitor of BRAF and EGFR that acts by inducing αC-helix-In and DFG-In conformation of protein (Karoulia et al., 2017; Tang et al., 2015). VEM is effective for constitutively active form of mutant BRAF^{V600E} protein, however, it can induce paradoxical RAF pathway activation due to negative allostery (Karoulia et al., 2017). BGB283 and inhibitors that favor the active or inward orientation of αC-helix and extended conformation of activation segment increase or stabilize BRAF-MEK1 complexes, whereas inhibitors like VEM orients αC-helix outwards and thereby inducing inactive conformation of the protein and weaken interaction of BRAF with MEK1 protein (Haling et al., 2014).

3.1. Structural differences between the ligand-free and ligand-bound conformations of BRAF^{WT} and BRAF^{V600E} protein

The simulated average structures were superimposed on each other to analyze the structural differences between apo and ligand bound structures. When BRAF^{WT} apo structure was superimposed on the BRAF^{WT}-ATP bound structure, it was found that ATP bound structure maintained active conformation by induing DGF-in and αC-helix-in conformation, while the opposite was found in the case of BRAF^{V600E} (Fig. 2A and B). Interestingly, when BRAF^{WT}-ATP bound structure was superimposed with BRAF^{WT-}Ponatinib, it was observed that DGF-in conformation was maintained by both the complexes, while αC-helix orientation was out in the case of Ponatinib-bound structure. Furthermore, DGF-out and αC-helix-out conformation was observed in both the structures of BRAF^{V600E} (Fig. 2C and D).

3.2. Structural insight into the effect of ponatinib, VEM and BGB283 on BRAF^{WT} and BRAF^{V600E} mutant on ATP-binding site

Active conformation of BRAF^{WT} dimer was obtained from BRAF-MEK1 dimer complex (PDB Id: 4MNE) and BRAF^{V600E} complexed with Ponatinib was retrieved from PDB having PDB ID 6P7G. Although the exact mechanism of action of BGB283, Ponatinib and VEM is known, molecular docking and MD simulations were carried out to get more insights into structural changes induced by these inhibitors on the selected crystallized structure of BRAF protein. VEM, BGB283 and

Table 1
Structural properties of BRAF^{WT}-Inhibitor dimer complexes and BRAF^{V600E} mutant-Inhibitor dimer complexes.

Parameters	MM-GBSA Binding energy (Kcal/mol)				DFG motif Conformation				αC-helix orientation				Binding Energy of two BRAF-MEK1 monomer
Protein-Inhibitor Complex	BRAF^{WT}		BRAF^{V600E}		BRAF^{WT}		BRAF^{V600E}		BRAF^{WT}		BRAF^{V600E}		BRAF^{WT}-MEK1 dimer
Chain	B	C	B	C	B	C	B	C	B	C	B	C	A-B:C-D
ATP					In	In	Out	Out	In	In	Out	Out	
BGB283	−49.71	−72.14	−103.85	−93.35	In	In	Out	Out	In	In	Out	In	−10.9
VEM	−62.28	−73.20	−84.69	−84.07	In	In	Out	Out	In	In	Out	In	−9.6
Ponatinib	−66.87	−78.33	−96.21	−106.27	In	In	Out	Out	Out	Out	Out	In	–
CAPE	−51.42	−57.36	−60.35	−60.37	In	In	Out	Out	In	In	Out	Out	−11.0
Wi-A	−40.23	−43.29	−39.91	−53.37	In	In	Out	Out	In	In	Out	In	−10.7
Wi-N	−50.14	−33.43	−33.36	−54.72	In	In	Out	Out	In	In	Out	In	−9.3

Table 2
Interactions formed by inhibitors with both chain B and C of BRAF^{WT} protein dimer. Interactions similar to that of interactions formed by BGB283 are highlighted in bold.

BRAF^{WT}-Inhibitor Complex	BRAF^{WT}-BGB283 complex		BRAF^{WT}-VEM complex		BRAF^{WT}-CAPE complex		BRAF^{WT}-Wi-A complex		BRAF^{WT}-Wi-N complex		BRAF^{WT}-Ponatinib complex	
Interactions	Chain B	Chain C	Chain B	Chain C	Chain B	Chain C	Chain B	Chain C	Chain B	Chain C	Chain B	Chain C
Hydrogen Bonds	Gly534	**Cys532** **Asn580**	**Ser536**	**Ser536** **Asp594**	Gln530			Ser536		**Thr470**	Glu533	
Hydrophobic interactions	**Ile463** **Gly464** **Gly466** **Val471** **Ala481** **Cys532** **Gly534** **Tyr538** **Ile543** **Phe583**	**Ile463** **Gly464** **Gly466** **Phe468** **Val471** **Ala481** **Trp531** **Cys532** **Gly534** **Tyr538** **Phe583**	Ile463 Gly464 Val471 Ala481 Cys532 Gly534 Phe583	Ile463 Phe468 **Gly469** Val471 Ala481 **Trp531** **Leu505** **Leu514** **Ile527** Gly534 Phe583 **Gly593** **Phe595**	Ile463 Gly464 Val471 Ala481 **Leu514** **Trp531** Cys532 Gly534 Phe583	Ile463 Gly464 Phe468 **Gly469** Val471 Ala481 **Leu514** Trp531 Cys532 Gly534 Phe583 **Leu584**	Ile463 Gly464 Val471 **Leu514** Cys532 Gly534 Tyr538 Ile543 Phe583	Ile463 Gly464 Phe468 **Gly469** Val471 Gly534 Phe583	Ile463 Gly464 Gly466 Val471 Ala481 **Leu514** **Trp531** Cys532 Gly534 Phe583	Phe468 **Gly469** **Met484** **Leu485** **Ala497** **Phe498**	Ile463 Val471 Ala481 Leu514 Ile543 Ile544 Phe583	Ile463 Val471 Tyr472 Ala481 Leu505 Leu514 Phe516 Ile527 Trp531 Cys532
Polar and Charged Interactions	**Ser465** **Ser467** **Ser535** **Ser536** **His539** **His585** **Asp594**	**Gln530** **Ser535** **Ser536** **His539** **Asn580**	Ser465 Ser535 Ser536 His539	**Ser467** **Glu533** **Thr529** Ser535 Ser536 **Asn580** **Asn581** **Asp594**	Ser465 **Thr529** Gln530 **Glu533** Ser535 His539 His585	**Ser465** **Thr529** Gln530 Ser535 **His585** **Lys591**	**Ser465** **Ser535** **Ser536** **His539** **His585**	Ser535 Ser536 His539 Asn580	Ser465 Ser467 **Lys483** **Thr529** **Gln530** Ser535 Ser536 His539 His585	**Thr470** **Lys483** **Gln494** **Lys578** Asn580	Lys483 **Thr529** Gln530 **Ser535** His539	**Arg462** Ser465 Lys473 Thr529 Lys483 **Gln530** **His539**
Pi-Pi Stacking		**Phe468**	**Trp531**	**Phe583**								Trp531

Ponatinib interacted at the ATP-binding site of both BRAF^{WT} and BRAF^{V600E} proteins and showed high binding affinity. VEM had −62.28 kcal/mol at chain B and −73.14 kcal/mol at chain C of BRAF^{WT}, it showed high binding affinity towards BRAF^{V600E,} i.e., −84.84 kcal/mol and −84.07 kcal/mol at chain B and C respectively. Further, BGB283 had −49.71 kcal/mol at chain B and −72.14 kcal/mol binding energy at chain C of BRAF^{WT} and similar binding energy was found at BRAF^{V600E,} i.e., −103.85 kcal/mol and −93.35 kcal/mol at chain B and C, respectively. Ponatinib showed lower binding with BRAF^{WT} (−66.87 & −78.33 kcal/mol) in comparison to BRAF^{V600E} (−96.21 & −106.27 kcal/mol). Although VEM is a well-known inhibitor of a constitutive active form of BRAF^{V600E}, it showed lower binding affinity as compared to that of BGB283. The orientation of αC-helix and DFG motifs were examined for all protein-ligand complexes to identify their possible mode of action (Table 1). It was found that VEM induced αC-helix-In and DFG-In orientation of BRAFWT and αC-helix-Out and DFG-out orientation of BRAFV600E protein (Table 1 and Fig. 3C, D, 3G and 3H). This finding was in line with other reports for BRAF^{V600E} protein. However, αC-helix-out conformation of BRAF^{WT} protein was not observed here (Fig. 3C and D). Further, Ponatinib showed the DFG-in conformation at both the chains, while αC-helix-in was observed at Chain B and αC-helix-out at chain C of BRAF^{WT}. In the case of BRAF^{V600E}, DGF-out conformation was observed at both the chains (Table 1 and Fig. 2).

Similarly, for BGB283, αC-helix-In and DGF-in, the extended activation segment and well-aligned hydrophobic R-spine residues (Leu505, Phe516, His574 and Phe595) were observed for BRAF^{WT} and out-conformation was found in BRAF^{V600E} (Fig. 3A, B, 3E and 3F) (Hu et al., 2015). The interactions formed by BGB283 and VEM at the ATP-binding site of BRAF^{WT} and BRAF^{V600E} mutant were also studied. Most of the interacting residues of VEM for both chains were the same as that of BGB283 in the case of BRAF^{WT} protein (Table 2). However, in the case of BRAF^{V600E} mutant, VEM forms interaction with different residues of the second chain, whereas, for the first chain, the majority of interacting residues were the same as that of BGB283 (Table 3). The protein-ligand RMSDs of all BRAF^{WT}-ligand complexes and BRAF^{V600E}--ligand complexes were also stable and comparable among all control and tested compounds (Fig. S1).

3.3. CAPE, Wi-A and Wi-N have potential to serve as ATP competitive inhibitors of BRAF^{WT} protein

The effect of test compounds (CAPE, Wi-A and Wi-N) was analyzed to understand structural alterations induced by them at the ATP-binding site of BRAF^{WT} protein. Molecular docking and MD simulations of these compounds with BRAF^{WT} protein were performed to get insight into various structural properties. It was observed that among test
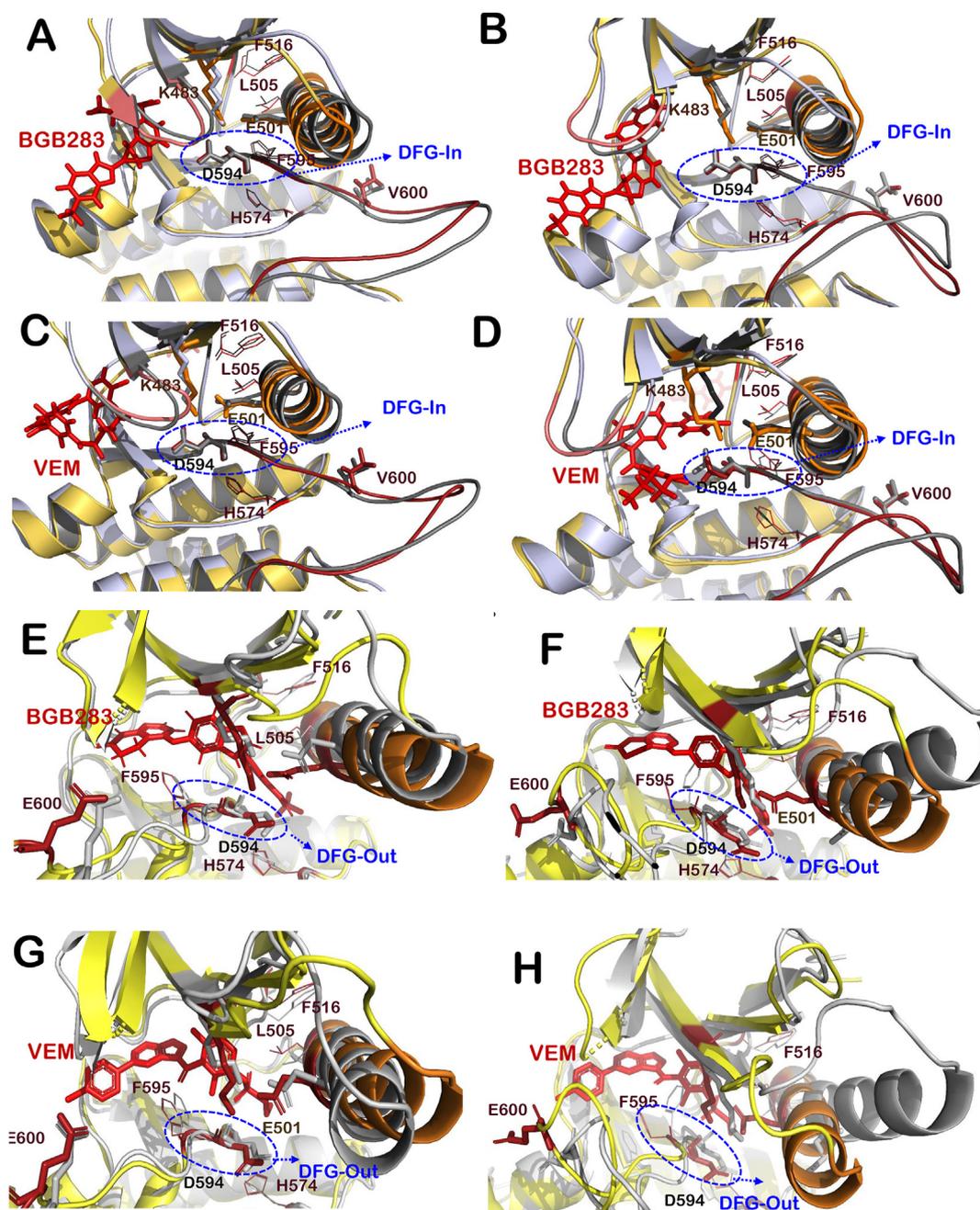
Fig. 3. Interaction of VEM and BGB283 at ATP-binding site of BRAF^WT and BRAF^V600E mutant. Superimposition of active BRAF^WT protein (grey) with BRAF^WT-BGB283 complex (yellow-red) at chain B (A) and chain C (B), BRAF^WT-VEM complex (yellow-red) at chain B (C) and chain C (D). Superimposition of BRAF^V600E protein structure (grey) with that of BRAF^V600E-BGB283 complex (yellow-red) at chain B (E) and chain C (F) and BRAF^V600E-VEM complex (yellow-red) at chain B (G) and chain C (H). The structural elements around ligand-binding site of BRAF^WT-inhibitor complex and BRAF^V600E-inhibitor complexes are highlighted that includes activation loop (shown in firebrick red color), αC-helix (orange), P loop (salmon) and R-spine residues (red lines representation). (For interpretation of the references to color in this figure legend, the reader is referred to the Web version of this article.)

compounds, CAPE was able to bind strongly with both chains (−51.42 and −57.36 kcal/mol) of BRAF^WT protein dimer (Table 1). Wi-A (−40.23 and −43.29 kcal/mol) and Wi-N (−50.14 and −33.43 kcal/mol) also showed a good binding affinity with both chains, however, binding energy was small in comparison to the control inhibitors (VEM and BGB283) (Table 1). The RMSD of CAPE (1.85 ± 1.23) was minimum followed by Wi-N (1.94 ± 0.64, BGB283 (2.38 ± 0.25), Wi-A (3.02 ± 0.55), and VEM (3.53 ± 0.63), however the binding of all the ligands was stable. The radius of gyration (Rg) that indicates the extendedness of the ligand in the binding pocket was investigated; it was found that Wi-A (23.34 ± 2.23) had the highest flexibility, followed by VEM (22.04 ±

2.39), Wi-N (21.22 ± 2.55), BGB283 (18.42 ± 2.35) and CAPE (15.92 ± 0.5). Further, CAPE (115.15 ± 48.23) was found to be more buried in the pocket than BGB283 (318.08 ± 32.80), Wi-N (347. ± 39.09), VEM (483.20 ± 45.20) and Wi-A (518.04 ± 49.78) through solvent accessible surface area calculations. Overall, these MD data showed that CAPE had maximum stability in the binding pocket amongst the three tested compounds. Other structural properties were analyzed for all BRAF^WT protein-ligand complexes. It was found that all the test compounds were able to maintain the active conformation of BRAF^WT protein dimer by induction of αC-helix-In, DFG-In, extended activation segment and well-aligned hydrophobic R-spine residues (Fig. 4A-F). Most of the

Table 3

Interactions formed by inhibitors with both chain B and C of BRAF^{V600E} mutant protein dimer. Interactions similar to that of interactions formed by BGB283 are highlighted in bold.

BRAF^{V600E} mutant-Inhibitor Complex	BRAF^{V600E} mutant -BGB283 complex		BRAF^{V600E} mutant -VEM complex		BRAF^{V600E} mutant -CAPE complex		BRAF^{V600E} mutant -Wi-A complex		BRAF^{V600E} mutant -Wi-N complex		BRAF^{V600E} mutant -Ponatinib complex	
Interactions	Chain B	Chain C	Chain B	Chain C	Chain B	Chain C	Chain B	Chain C	Chain B	Chain C	Chain B	Chain C
Hydrogen Bonds	Glu501 Cys532	Asn580	Asp594 Phe595		GLN530 Cys532	**Cys532** **Asp594**	His574	**Gln609**			**Glu501** His 574	**Glu501** **His574** **Asp594**
Hydrophobic interactions	**Ile463** **Gly464** **Gly466** **Val471** **Ala481** **Leu514** **Trp531** **Cys532** **Gly534** **Phe583**	**Phe468** **Gly469** **Val471** **Ala481** **Leu514** **Tyr538** **Phe583** **Gly593** **Trp619**	Ile463 Gly464 Val471 Ala481 **Val482** **Leu505** Leu514 **Ile527** **Val528** Cys532 Phe583 **Gly593** **Phe595**	**Ile463** **Gly464** **Trp531**	Ile463 Val471 Ala481 **Leu505** **Ile513** Leu514 Leu515 Leu516 **Ile527** Trp531 Cys532 Phe583 Gly593 **Phe595**	Ile463 Val471 Ala481 Leu514 **Trp531** **Cys532** Phe583 Phe595 Phe597	Ile463 Gly464 Gly466 Val471 Ala481 Leu514 Cys532 Gly534 Phe583 Gly593 Phe595	Gly464 **Val504** **Leu505** **Leu567** **Ile572** **Ile573** **Tyr633**	Val504 Leu505 Ile513 Leu514 Leu567 Ile572 Ile573 Ile592	Val504 Leu505 Ile513 Leu514 Leu567 Ile572 Ile573 Ile592	Ile463 Val471 Ala481 Val482 Ala497 Val504 Leu505 Ile527 Val528 Ile572 Ile573	Ile463 Val471 Ala481 Val482 Ala497 Val504 Leu505 Ile527 Val528 Ile573 Ile592
Polar and Charged Interactions	**Ser465** **Lys483** **Thr529** **Glu533** **Ser535** **Ser536** **Asp594**	**Ser467** **Lys483** **Thr529** **Lys578** **Asn580** **Asn581** **Asp594**	Ser465 Lys483 **Glu501** Thr529 **Asn580** **Asn581** Asp594 **Ser616**	**Gln461** **Arg462** **Ser465** **Lys473**	Lys483 Thr529 Thr529 **Gln530** Asp594	Ser467 Lys483 Thr529 Gln530 **Ser535** **Ser536** **His539** Asn580 Asp594	Lys507 Thr508 His574 Arg575	**Asn500** **Glu501** **Thr508** **Arg575** **Asn581** **His608** **Gln612**	Glu501 Thr508 His514 Arg575 Asp594	**His574** **Gln496** **Asn500** **Glu501** **Thr508** **Asp594** **His608** Asn580	**Thr529** **Gln530** **Asp594** **Glu501** **Asp576**	**Lys483** **Asn500** **Arg575** **Asp576**
Pi-Pi Stacking					**Phe468**						**Phe595**	**Phe595**

interactions formed by CAPE and Wi-A with both chains of protein dimer were common for both BGB283 and VEM, whereas for Wi-N interactions formed at chain B were similar but different at chain C (Table 2). When significant hydrogen bond interactions (more than 30% of the time of the simulation) were analyzed, it was found that three compounds were comparable in terms of number as well as consistency of polar and non-polar interactions with positive controls throughout the simulations, as shown in Fig. S2.

The binding energy for Ras-induced BRAF-MEK1 complexes dimerization was also calculated in the presence of various inhibitors. The binding energy of ATP-bound BRAF-MEK1 monomer with another ATP-bound BRAF-MEK1 monomer was calculated as −10.6 kcal/mol. BGB283 caused an increase in the binding energy of these complexes, whereas in the case of VEM, a slight decrease in binding energy was observed (Table 1). Both CAPE and Wi-A increased the binding energy of BRAF-MEK1 complexes for hetero-tetramer formation, just like BGB283. On the other hand, just like VEM, Wi-N caused a decrease in the binding energy of two BRAF-MEK1 monomers (Table 1).

3.4. Tested natural compounds have potential to serve as ATP competitive inhibitors of BRAF^{V600E} mutant protein

In the case of BRAF^{V600E}, when MD trajectories were analyzed, it was found that the three compounds; Wi-A (2.41 ± 0.63 Å), Wi-N (1.95 ± 0.57 Å) and CAPE (1.32 ± 0.16 Å), had similar fluctuations as VEM (1.12 ± 0.26 Å), BGB283 (0.75 ± 0.1 Å) and Ponatinib (1.12 ± 0.20) in RMSD calculations. The Radius of Gyration value of Wi-A (18.65 ± 2.59 Å) was the highest followed by Wi-N (17.03 ± 0.49 Å), Ponatinib (15.62 ± 1.16 Å), VEM (14.93 ± 0.19 Å), CAPE (14.72 ± 0.20 Å) and BGB283 (13.95 ± 0.13 Å). Further, solvent accessible surface area calculation showed that BGB283 (55.18 ± 6.57Å^2) was least accessible to solvent, followed by CAPE (107.80 ± 13.94 Å^2), VEM (181.10 ± 24.34 Å^2), Ponatinib (181.91 ± 30.45 Å^2), Wi-N (326.09 ± 36.93 Å^2) and Wi-A (443.52 ±

53.71 Å^2). Overall dynamics data again suggested that in all the natural compounds studied, CAPE binding was stable with V600E mutant similar to BRAF^{WT}. Further insight into the conformational analysis of structures suggested that VEM induces αC-out conformation of the protein (Fig. 3G and H). Similarly, All three compounds induce the DGF-out and αC-helix-out in BRAF^{V600E} except in the case of Chain C where Wi-A and Wi-N caused αC-helix-in conformation. (Fig. 5A-E). Moreover, CAPE showed stronger (−67.35 and −60.67 kcal/mol) binding at ATP-binding site as compared to Wi-N (−33.36 and −54.72 kcal/mol), and Wi-A (−39.91 and −53.37 kcal/mol) (Table 1). As observed in the case of BRAF^{WT}-inhibitor complexes, most of the interactions formed by the test compounds with BRAF^{V600E} mutant were similar to interactions formed by BGB283 (Table 3). Specifically, when significant hydrogen bond interactions (more than 30% of the simulation time) between the compounds and BRAF^{V600E} mutant were investigated, it was found that at Chain B, Lys483 and Asp594 were common significant interactive residues with Ponatinib, CAPE and Wi-A. On the other hand, Glu501 was common among Wi-N, BGB283 and VEM and, Asp594 was common between Wi-A VEM and CAPE. Further, Ser467 was making crucial interaction in the case of Wi-N. While Asn594 was common in Ponatinib, VEM, Wi-A, Wi-N and CAPE at chain C. (Fig. S3).

4. Discussion

Constitutive high expression and mutations in BRAF are the common root cause of various cancers such as Melanoma (27–60%), papillary thyroid cancer (36–69%) and colon cancer (5–17%) (Crispo et al., 2019). Various small molecule inhibitors have been investigated in the past against wild type and mutant BRAF proteins. Sorafenib was first clinically evaluated and found to be a broad-spectrum inhibitor of various kinases. However, due to lack of mutant-based efficacy and specificity, this drug was ineffective against melanoma patients (Ascierto et al., 2012). Further, two BRAF mutant specific (V600E) drugs, VEM and dabrafenib,
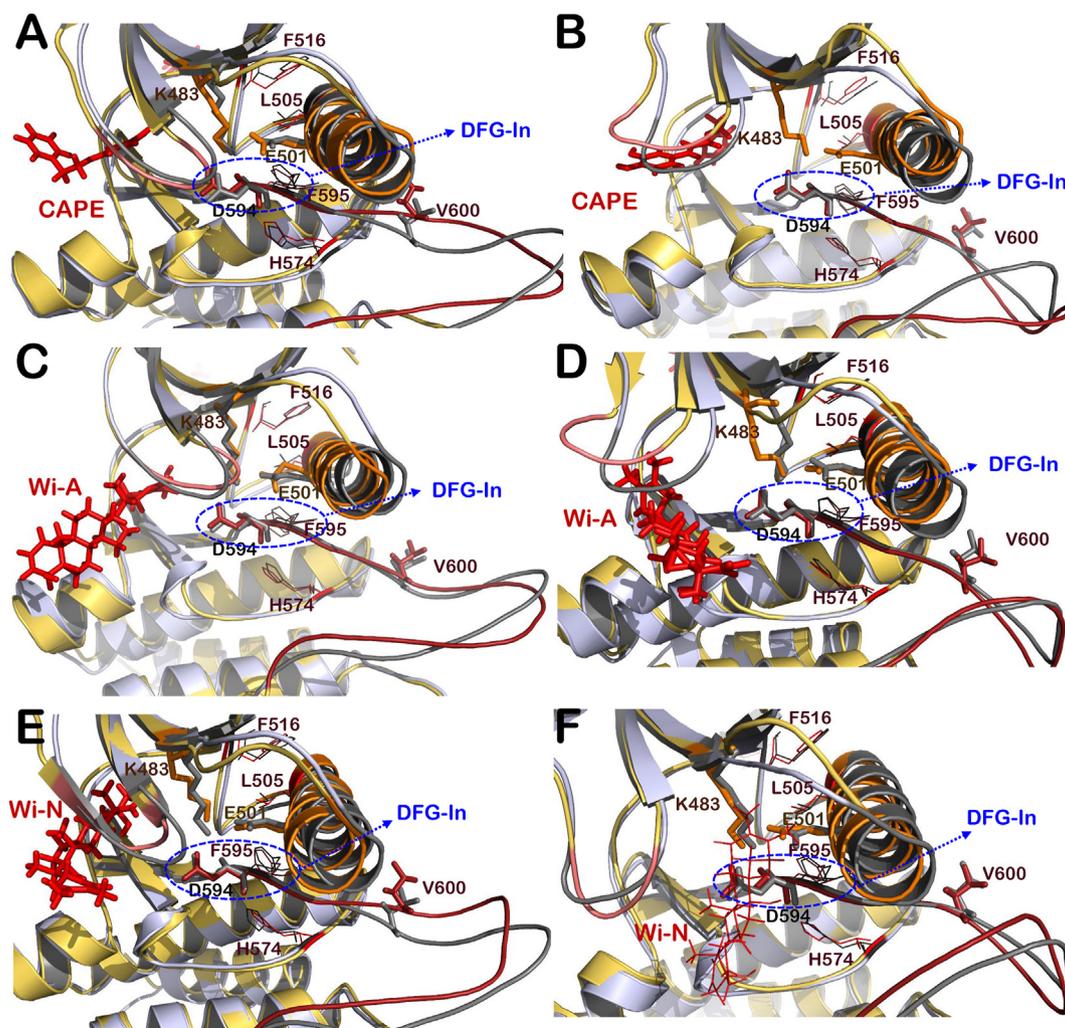
Fig. 4. Interaction of CAPE, Wi-A and Wi-N at ATP-binding site of BRAF^{WT} protein. Superimposition of active BRAF^{WT} protein (grey) with BRAF^{WT}-Inhibitor complexes (yellow-red) including BRAF-CAPE complex at chain B (A) and chain C (B), BRAF-Wi-A complex at chain B (C) and chain C (D) and BRAF-Wi-N complex at chain B (E) and chain C (F). Structural elements of BRAF^{WT}-inhibitor complexes like activation segment (shown in firebrick color), αC-helix (orange), P loop (salmon) and R-spine residues (red lines representation). (For interpretation of the references to color in this figure legend, the reader is referred to the Web version of this article.)

were approved. They showed significant response and survival rate in BRAF-related cancer patients (Sanchez et al., 2018). In spite of early success, it was found later that cancer cells got resistant to these medications in a span of a few months to a year (Villanueva et al., 2011). Further, a novel class inhibitor BGB283 was reported to have a remarkable response in pre-clinical as well as 1st phase of the clinical trial. In 1st phase clinical trial study, it was found that BGB283 possess an acceptable risk benefit profile and was found effective against BRAF^{V600E} mutant patients with melanoma, papillary thyroid cancer NSCLC and others (Desai et al., 2020). However, its efficacy/safety profile and comparison with first class inhibitors are still not well studied and need to be evaluated. However, the resistance of cancer cells against a single therapeutic agent and side-effects of multiple therapeutics in cancer patients have triggered interest and investigations on natural compounds. Here, we studied three natural compounds, CAPE, Wi-A and Wi-N, against BRAF autophosphorylation. Wi-A has been shown to inhibit the cancer cells with and without telomerase by myc-mad transcriptional suppression of MRN complex proteins (Yu et al., 2017). Wi-A has also been shown to suppress the growth and migration of hepatocellular carcinoma in mice (Siddharth et al., 2019). Interestingly, Wi-A with a combination of Sorafenib has been reported to show a dose-dependent synergistic effect for the downregulation of BRAF (Cohen et al., 2012). Further, Wi-N rich

ashwagandha alcoholic extract has been reported to restrict metastasis and angiogenesis by downregulating migration promoting proteins (Gao et al., 2014). CAPE has also been reported to be effective against melanoma, lung, prostate and breast cancer in pre-clinical studies (Ozturk et al., 2012).

The previously reported *in vivo* and *in vitro* studies indicated the anticancer potential of these natural compounds on BRAF or EGFR-related cancer, however, their mechanism of action has not been resolved (Cohen et al., 2012; Choromanska et al., 2020; Dutta et al., 2019; Wu et al., 2011; Kunimasa et al., 2017). Our previously published computational study explored the ATP-competitive potential of test compounds for different mutant forms of EGFR (Malik et al., 2021). The provided *in silico* evidence suggested that Wi-A and Wi-N could serve as ATP-competitive inhibitors of wild type, L858R, exon 19 deletion and exon 20 insertion mutants (D770_N771^{InsNPG}, D770_N771^{InsSVD}, V769_D770^{InsASV} and H773_V774^{InsH}), while CAPE could bind effectively against wild type and exon20 insertion mutants of EGFR only. Hence, *in silico* experiments were performed to check the ATP-competitive potential of test compounds against BRAF^{WT} and BRAF^{V600E} mutant to check if they can serve as a dual inhibitor of EGFR and BRAF similar to BGB283 and ponatinib. *In silico* techniques like molecular docking, MD simulation, MM/GBSA free binding energy calculations were used to examine
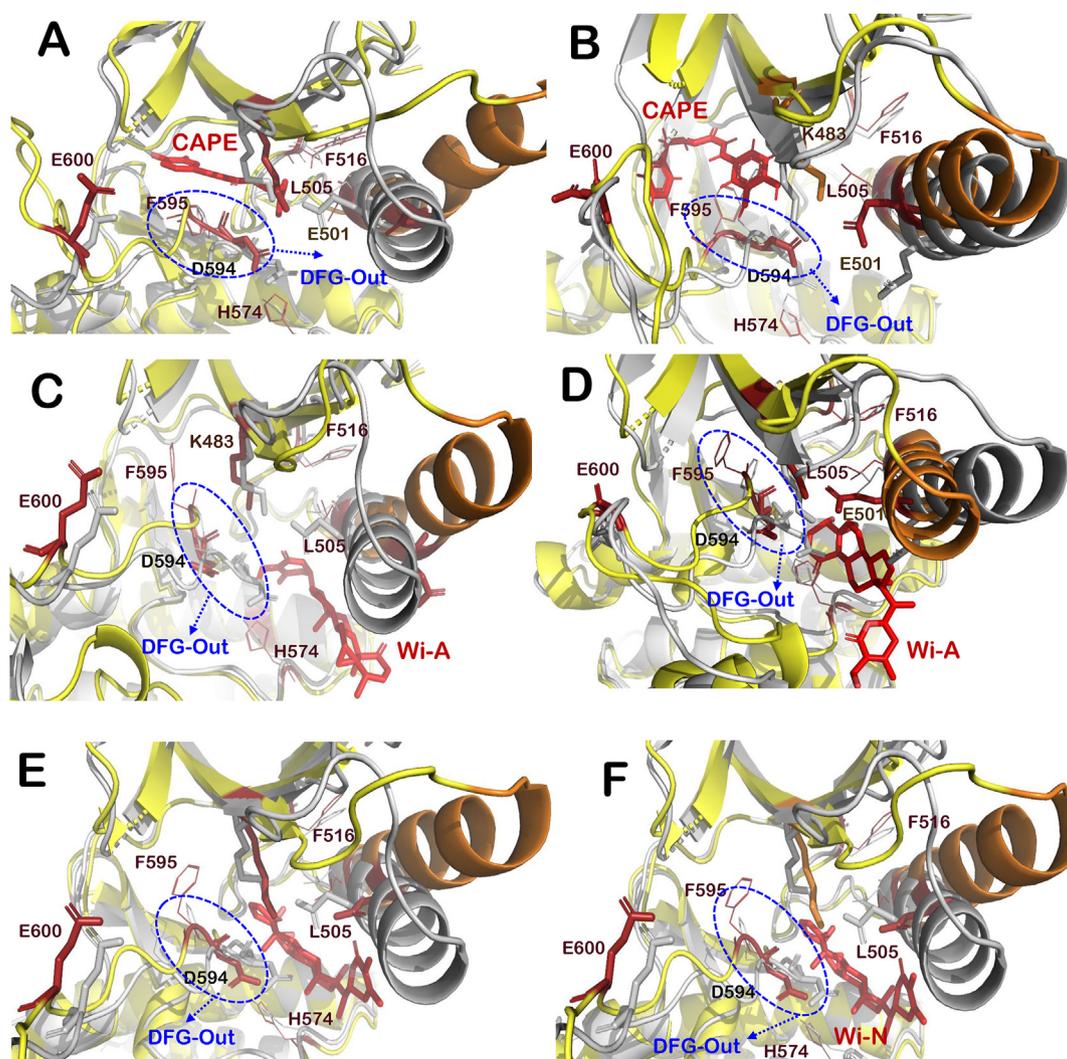
Fig. 5. Interaction of CAPE, Wi-A and Wi-N at ATP binding site of BRAF^{V600E} mutant protein. Superimposition of BRAF^{V600E} protein structure (grey) with that of BRAF^{V600E} mutant-Inhibitor complexes (yellow-red) including BRAF-CAPE complex at chain B (A) and chain C (B), BRAF-Wi-A complex at chain B (C) and chain C (D) and BRAF-Wi-N complex at chain B (E) and chain C (F). Structural elements of BRAF^{V600E}-inhibitor complexes like activation segment (shown in firebrick color), αC-helix (orange), P loop (salmon) and R-spine residues (red lines representation). Helical turn introduced in activation segment of BRAF^{V600E}-Wi-N complex is highlighted with cyan colored circle. (For interpretation of the references to color in this figure legend, the reader is referred to the Web version of this article.)

the potential of test compounds to serve as ATP-competitive inhibitors of cancers caused by constitutive activation or mutations of BRAF. It was found that all the three test compounds (CAPE, Wi-A and Wi-N) could stably interact at the ATP-binding site of both BRAF^{WT} and BRAF^{V600E} mutant protein and form interactions with similar interacting residues of already reported inhibitors (VEM and BGB283). In the case of BRAF^{WT}, all test and control inhibitors maintained the active conformation of the protein by inducing DFG-In, αC-helix-In and extended conformation of the activation segment. However, VEM induced inactive conformation of BRAF^{V600E} by inducing DFG-In, αC-helix-Out and extended activation segment. Similarly, All the natural compounds also induced inactive conformation of protein via introduction of helical turn in activation segment and maintaining DFG-out and αC-helix-out conformation. Therefore, it can be deciphered that like BGB283, active conformation was maintained by all test and control compounds in the case of BRAF^{WT}, thereby may prevent paradoxical activation of protein due to negative allostery and strengthen BRAF-MEK complexes. This was in line with protein-protein binding energy calculations that showed that both Wi-A and CAPE strengthen BRAF-MEK complexes like BGB283. However, Wi-N binding with BRAF^{WT} resulted in the decreased binding energy of BRAF with MEK, as it was observed in the case of VEM (Table 1). Among

CAPE and Wi-A, CAPE showed stronger and deeper binding in the ATP-binding pocket of BRAF^{WT} as well as BRAF^{V600E}.

The approximation and parameterization of atomic-level forces are the main limitations of the different force fields, which may further lead to variations in the ensemble generated by the simulation (Wang and O'Mara, 2021). In the current study, different force field effects have not been investigated on the studied systems, but only a well-known force field for protein and small molecules, i.e., OPLS3e, has been used throughout the study (Roos et al., 2019) (Dhanjal et al., 2021). Although OPLS3e is the most updated forcefield used nowadays, other popular force fields like AMBER, CHARMM, and GROMOS are also available (Guvench and MacKerell, 2008). Replicates of simulations were not required, as all the conditions and parameters, including the initial seed value for velocity randomization was set to a custom value (initial seed value = 2007). To confirm the reproducibility of the simulation results, five replicates of BRAF^{WT} – Ponatinib complex were simulated under identical conditions, which showed highly similar trajectories (data not shown). Further, the calculated MM/GBSA protein-ligand binding energies do not represent absolute binding energies due to ignorance of entropy changes and the use of implicit solvation models (Mulakala and Viswanadhan, 2013; Genheden and Ryde, 2015). Therefore, all the

MM/GBSA protein-ligand binding energies reported in this study represent the relative binding affinity of ligands to the protein with respect to each other. Also, all the protein-ligand complexes studied were simulated for a time duration of 100 ns only. To better understand our protein-ligand systems in terms of stability and time required to attain conformational changes upon ligand binding, one protein-ligand systems (BRAF^WT-VEM dimer) was simulated for 500ns. The RMSD plots of protein and ligand complexes clearly showed that the systems had attained stability within 50 ns of simulation (Fig. S4A). The average representative structures of the complex were attained from stable trajectories of initial 50 ns and 500 ns simulation, respectively, and compared to check the stability of the ligand at the ATP-binding pocket (Fig. S4B). This provided us a clear understanding of the behavior of our protein-ligand complexes during MD simulation and aided in deciding the duration of simulation required to attain stability for the rest of the systems. Our *in silico* study suggested that Wi-A, Wi-N and CAPE could serve as ATP competitive inhibitors in the case of treatment of cancer with aberrant BRAF activity or BRAF^V600E mutations. However, *in vitro* and *in vivo* experimental validation of the potential of these compounds to serve as dual inhibitor in cancer with aberrant EGFR and BRAF activity will confirm their mechanism of action.

5. Conclusion

The effect of natural compounds CAPE, Wi-A and Wi-N as competitive inhibitors of ATP binding site of BRAF^WT and BRAF^V600E mutant was explored in this study. Ponatinib (FDA approved drug that targets multiple receptor tyrosine kinases), VEM (FDA approved drug for BRAF^V600E mutant) and BGB283 (a dual inhibitor of BRAF and EGFR) were taken as control. It was concluded that the three natural compounds have potential to serve as ATP competitive inhibitors of BRAF^WT and BRAF^V600E proteins by favoring their active conformation, except for Wi-N induced inactive conformation in the case of BRAF^V600E mutant protein. Although Wi-N did not completely resemble VEM's action mechanism, it induced inactive conformation of activation segment in one of the chains of BRAF^V600E mutant dimer. It also followed the same pattern of change in the binding energy of BRAF-MEK1 complexes dimerization as observed in the case of VEM. Although all three natural compounds may serve as inhibitors of BRAF^WT and BRAF^V600E, CAPE showed a higher binding affinity with BRAF^WT protein and BRAF^V600E protein compared to other studied ligands. Collectively, we have shown the crucial interactive residues, energetics, and binding mechanism of the three natural compounds against BRAF proteins, which can be helpful in providing the mechanistic insights of BRAF inhibition. However, experimental validation is required to confirm the findings of the study for its application in rational drug design.

CRediT authorship contribution statement

Vidhi Malik: Conceptualization, Design, Formal analysis, Manuscript writing. **Vipul Kumar:** Formal analysis, Manuscript writing. **Sunil C. Kaul:** Conceptualization, Design, Manuscript writing. **Renu Wadhwa:** Conceptualization, Design, Manuscript writing. **Durai Sundar:** Conceptualization, Design, Manuscript writing.

Declaration of competing interest

The authors declare that they have no known competing financial interests or personal relationships that could have appeared to influence the work reported in this paper.

Acknowledgments

Appendix A. Supplementary data

Supplementary data to this article can be found online at https://doi.org/10.1016/j.crstbi.2021.11.004.

References

Ascierto, P.A., Kirkwood, J.M., Grob, J.J., Simeone, E., Grimaldi, A.M., Maio, M., Palmieri, G., Testori, A., Marincola, F.M., Mozzillo, N., 2012. The role of BRAF V600 mutation in melanoma. J. Transl. Med. 10, 85. https://doi.org/10.1186/1479-5876-10-85.

Avruch, J., Khokhlatchev, A., Kyriakis, J.M., Luo, Z., Tzivion, G., Vavvas, D., Zhang, X.F., 2001. Ras activation of the Raf kinase: tyrosine kinase recruitment of the MAP kinase cascade. Recent Prog. Horm. Res. 56, 127–155. https://doi.org/10.1210/rp.56.1.127.

Ballantyne, A.D., Garnock-Jones, K.P., 2013. Dabrafenib: first global approval. Drugs 73, 1367–1376. https://doi.org/10.1007/s40265-013-0095-2.

Choromanska, A., Saczko, J., Kulbacka, J., 2020. Caffeic acid phenethyl ester assisted by reversible electroporation-in vitro study on human melanoma cells. Pharmaceutics 12. https://doi.org/10.3390/pharmaceutics12050478.

Cohen, S.M., Mukerji, R., Timmermann, B.N., Samadi, A.K., Cohen, M.S., 2012. A novel combination of withaferin A and sorafenib shows synergistic efficacy against both papillary and anaplastic thyroid cancers. Am. J. Surg. 204, 895–900. https://doi.org/10.1016/j.amjsurg.2012.07.027 discussion 900-891.

Cotto-Rios, X.M., Agianian, B., Gitego, N., Zacharioudakis, E., Giricz, O., Wu, Y., Zou, Y., Verma, A., Poulikakos, P.I., Gavathiotis, E., 2020. Inhibitors of BRAF dimers using an allosteric site. Nat. Commun. 11, 4370. https://doi.org/10.1038/s41467-020-18123-2.

Crispo, F., Notarangelo, T., Pietrafesa, M., Lettini, G., Storto, G., Sgambato, A., Maddalena, F., Landriscina, M., 2019. BRAF inhibitors in thyroid cancer: clinical impact, mechanisms of resistance and future perspectives. Cancers 11. https://doi.org/10.3390/cancers11091388.

Croce, L., Coperchini, F., Magri, F., Chiovato, L., Rotondi, M., 2019. The multifaceted anti-cancer effects of BRAF-inhibitors. Oncotarget 10, 6623–6640. https://doi.org/10.18632/oncotarget.27304.

Delord, J.P., Robert, C., Nyakas, M., McArthur, G.A., Kudchakar, R., Mahipal, A., Yamada, Y., Sullivan, R., Arance, A., Kefford, R.F., et al., 2017. Phase I dose-escalation and -expansion study of the BRAF inhibitor Encorafenib (LGX818) in metastatic BRAF-mutant melanoma. Clin. Cancer Res. : J. Am. Assoc. Cancer Res. 23, 5339–5348. https://doi.org/10.1158/1078-0432.CCR-16-2923.

Desai, J., Gan, H., Barrow, C., Jameson, M., Atkinson, V., Haydon, A., Millward, M., Begbie, S., Brown, M., Markman, B., et al., 2020. Phase I, open-label, dose-escalation/dose-expansion study of lifirafenib (BGB-283), an RAF family kinase inhibitor, in patients with solid tumors. J. Clin. Oncol. : J. Am. Soc. Clin. Oncol. 38, 2140–2150. https://doi.org/10.1200/JCO.19.02654.

Dhanjal, J.K., Kumar, V., Garg, S., Subramani, C., Agarwal, S., Wang, J., Zhang, H., Kaul, A., Kalra, R.S., Kaul, S.C., et al., 2021. Molecular mechanism of anti-SARS-CoV2 activity of Ashwagandha-derived withanolides. Int. J. Biol. Macromol. 184, 297–312. https://doi.org/10.1016/j.ijbiomac.2021.06.015.

Diukendjieva, A., Zaharieva, M.M., Mori, M., Alov, P., Tsakovska, I., Pencheva, T., Najdenski, H., Kren, V., Felici, C., Bufalieri, F., et al., 2020. Dual SMO/BRAF inhibition by flavonolignans from Silybum marianum (dagger). Antioxidants 9. https://doi.org/10.3390/antiox9050384.

Dutta, R., Khalil, R., Green, R., Mohapatra, S.S., Mohapatra, S., 2019. Withania somnifera (ashwagandha) and withaferin A: potential in integrative oncology. Int. J. Mol. Sci. 20. https://doi.org/10.3390/ijms20215310.

Fofaria, N.M., Ramachandran, S., Srivastava, S.K., 2017. Therapeutic potential of black pepper compound for BRaf resistant melanoma. Proceedings 1, 981.

Friesner, R.A., Murphy, R.B., Repasky, M.P., Frye, L.L., Greenwood, J.R., Halgren, T.A., Sanschagrin, P.C., Mainz, D.T., 2006. Extra precision glide: docking and scoring incorporating a model of hydrophobic enclosure for protein– ligand complexes. J. Med. Chem. 49, 6177–6196.

Gao, R., Shah, N., Lee, J.S., Katiyar, S.P., Li, L., Oh, E., Sundar, D., Yun, C.O., Wadhwa, R., Kaul, S.C., 2014. Withanone-rich combination of Ashwagandha withanolides restricts metastasis and angiogenesis through hnRNP-K. Mol. Cancer Therapeut. 13, 2930–2940. https://doi.org/10.1158/1535-7163.MCT-14-0324.

Genheden, S., Ryde, U., 2015. The MM/PBSA and MM/GBSA methods to estimate ligand-binding affinities. Expet Opin. Drug Discov. 10, 449–461. https://doi.org/10.1517/17460441.2015.1032936.

Gentilcore, G., Madonna, G., Mozzillo, N., Ribas, A., Cossu, A., Palmieri, G., Ascierto, P.A., 2013. Effect of dabrafenib on melanoma cell lines harbouring the BRAF(V600D/R) mutations. BMC Cancer 13, 17. https://doi.org/10.1186/1471-2407-13-17.

Grasso, M., Estrada, M.A., Ventocilla, C., Samanta, M., Maksimoska, J., Villanueva, J., Winkler, J.D., Marmorstein, R., 2016. Chemically linked Vemurafenib inhibitors promote an inactive BRAF(V600E) conformation. ACS Chem. Biol. 11, 2876–2888. https://doi.org/10.1021/acschembio.6b00529.

Guvench, O., MacKerell Jr., A.D., 2008. Comparison of protein force fields for molecular dynamics simulations. Methods Mol. Biol. 443, 63–88. https://doi.org/10.1007/978-1-59745-177-2_4.

Haling, J.R., Sudhamsu, J., Yen, I., Sideris, S., Sandoval, W., Phung, W., Bravo, B.J., Giannetti, A.M., Peck, A., Masselot, A., et al., 2014. Structure of the BRAF-MEK complex reveals a kinase activity independent role for BRAF in MAPK signaling. Cancer Cell 26, 402–413. https://doi.org/10.1016/j.ccr.2014.07.007.

Holderfield, M., Deuker, M.M., McCormick, F., McMahon, M., 2014. Targeting RAF kinases for cancer therapy: BRAF-mutated melanoma and beyond. Nat. Rev. Cancer 14, 455–467. https://doi.org/10.1038/nrc3760.

Hu, J., Ahuja, L.G., Meharena, H.S., Kannan, N., Kornev, A.P., Taylor, S.S., Shaw, A.S., 2015. Kinase regulation by hydrophobic spine assembly in cancer. Mol. Cell Biol. 35, 264–276. https://doi.org/10.1128/MCB.00943-14.

Huang, M., Lu, J.J., Ding, J., 2021. Natural products in cancer therapy: past, present and future. Nat. Prod. Bioprospecting 11, 5–13. https://doi.org/10.1007/s13659-020-00293-7.

Humphrey, W., Dalke, A., Schulten, K., 1996. VMD - visual molecular dynamics. J. Mol. Graph. 14, 33–38.

Ichikawa, H., Takada, Y., Shishodia, S., Jayaprakasam, B., Nair, M.G., Aggarwal, B.B., 2006. Withanolides potentiate apoptosis, inhibit invasion, and abolish osteoclastogenesis through suppression of nuclear factor-kappaB (NF-kappaB) activation and NF-kappaB-regulated gene expression. Mol. Cancer Therapeut. 5, 1434–1445. https://doi.org/10.1158/1535-7163.MCT-06-0096.

Karoulia, Z., Gavathiotis, E., Poulikakos, P.I., 2017. New perspectives for targeting RAF kinase in human cancer. Nat. Rev. Cancer 17, 676–691. https://doi.org/10.1038/nrc.2017.79.

King, A.J., Arnone, M.R., Bleam, M.R., Moss, K.G., Yang, J., Fedorowicz, K.E., Smitheman, K.N., Erhardt, J.A., Hughes-Earle, A., Kane-Carson, L.S., et al., 2013. Dabrafenib; preclinical characterization, increased efficacy when combined with trametinib, while BRAF/MEK tool combination reduced skin lesions. PLoS One 8, e67583. https://doi.org/10.1371/journal.pone.0067583.

Kumar, V., Singh, J., Hasnain, S.E., Sundar, D., 2021. Possible link between higher transmissibility of alpha, Kappa and delta variants of SARS-CoV-2 and increased structural stability of its spike protein and hACE2 affinity. Int. J. Mol. Sci. 22. https://doi.org/10.3390/ijms22179131.

Kunimasa, K., Nagano, T., Shimono, Y., Dokuni, R., Kiriu, T., Tokunaga, S., Tamura, D., Yamamoto, M., Tachihara, M., Kobayashi, K., et al., 2017. Glucose metabolism-targeted therapy and withaferin A are effective for epidermal growth factor receptor tyrosine kinase inhibitor-induced drug-tolerant persisters. Cancer Sci. 108, 1368–1377. https://doi.org/10.1111/cas.13266.

Malik, V., 2020. Molecular Targets for Cancer Therapeutics: Insights from Genomic Aberrations and Protein Interactions. Doctoral thesis. Indian Institute of Technology, Delhi.

Malik, V.K.V., Kaul, S.C., Wadhwa, R., Sundar, D., 2021. Computational insights into the potential of withaferin-A, Withanone and caffeic acid phenethyl ester for treatment of aberrant-EGFR driven lung cancers. Biomolecules 11, 160. https://doi.org/10.3390/biom11020160.

Mulakala, C., Viswanadhan, V.N., 2013. Could MM-GBSA be accurate enough for calculation of absolute protein/ligand binding free energies? J. Mol. Graph. Model. 46, 41–51. https://doi.org/10.1016/j.jmgm.2013.09.005.

Muller, M.C., Cervantes, F., Hjorth-Hansen, H., Janssen, J., Milojkovic, D., Rea, D., Rosti, G., 2017. Ponatinib in chronic myeloid leukemia (CML): consensus on patient treatment and management from a European expert panel. Crit. Rev. Oncol.-Hematol. 120, 52–59. https://doi.org/10.1016/j.critrevonc.2017.10.002.

Munoz-Couselo, E., Garcia, J.S., Perez-Garcia, J.M., Cebrian, V.O., Castan, J.C., 2015. Recent advances in the treatment of melanoma with BRAF and MEK inhibitors. Ann. Transl. Med. 3, 207. https://doi.org/10.3978/j.issn.2305-5839.2015.05.13.

Newman, D.J., Cragg, G.M., 2016. Natural products as sources of new drugs from 1981 to 2014. J. Nat. Prod. 79, 629–661. https://doi.org/10.1021/acs.jnatprod.5b01055.

Newman, D.J., Cragg, G.M., 2020. Natural products as sources of new drugs over the nearly four decades from 01/1981 to 09/2019. J. Nat. Prod. 83, 770–803. https://doi.org/10.1021/acs.jnatprod.9b01285.

Nishikawa, Y., Okuzaki, D., Fukushima, K., Mukai, S., Ohno, S., Ozaki, Y., Yabuta, N., Nojima, H., 2015. Withaferin A induces cell death selectively in androgen-independent prostate cancer cells but not in normal fibroblast cells. PLoS One 10, e0134137. https://doi.org/10.1371/journal.pone.0134137.

Ozturk, G., Ginis, Z., Akyol, S., Erden, G., Gurel, A., Akyol, O., 2012. The anticancer mechanism of caffeic acid phenethyl ester (CAPE): review of melanomas, lung and prostate cancers. Eur. Rev. Med. Pharmacol. Sci. 16, 2064–2068.

Proietti, I., Skroza, N., Michelini, S., Mambrin, A., Balduzzi, V., Bernardini, N., Marchesiello, A., Tolino, E., Volpe, S., Maddalena, P., et al., 2020. BRAF inhibitors:

molecular targeting and immunomodulatory actions. Cancers 12. https://doi.org/10.3390/cancers12071823.

D. E. Shaw Research, New York, NY Protein Preparation Wizard, Epik, Impact, Prime, LigPrep, Glide, SiteMap, Desmond Molecular Dynamics System, 2018. Maestro-Desmond Interoperability Tools, Schrödinger, New York, NY, 2018., 2; Schrödinger Release 2018-4.

Roos, K., Wu, C., Damm, W., Reboul, M., Stevenson, J.M., Lu, C., Dahlgren, M.K., Mondal, S., Chen, W., Wang, L., et al., 2019. OPLS3e: extending Force Field Coverage for Drug-Like Small Molecules. J. Chem. Theor. Comput. 15, 1863–1874. https://doi.org/10.1021/acs.jctc.8b01026.

Sanchez, J.N., Wang, T., Cohen, M.S., 2018. BRAF and MEK inhibitors: use and resistance in BRAF-mutated cancers. Drugs 78, 549–566. https://doi.org/10.1007/s40265-018-0884-8.

Sari, A.N., Bhargava, P., Dhanjal, J.K., Putri, J.F., Radhakrishnan, N., Shefrin, S., Ishida, Y., Terao, K., Sundar, D., Kaul, S.C., et al., 2020. Combination of withaferin-A and CAPE provides superior anticancer potency: bioinformatics and experimental evidence to their molecular targets and mechanism of action. Cancers 12. https://doi.org/10.3390/cancers12051160.

Savoia, P., Fava, P., Casoni, F., Cremona, O., 2019. Targeting the ERK signaling pathway in melanoma. Int. J. Mol. Sci. 20. https://doi.org/10.3390/ijms20061483.

Shirley, M., 2018. Encorafenib and binimetinib: first global approvals. Drugs 78, 1277–1284. https://doi.org/10.1007/s40265-018-0963-x.

Siddharth, S., Muniraj, N., Saxena, N.K., Sharma, D., 2019. Concomitant inhibition of cytoprotective autophagy augments the efficacy of withaferin A in hepatocellular carcinoma. Cancers 11. https://doi.org/10.3390/cancers11040453.

Tan, F.H., Putoczki, T.L., Stylli, S.S., Luwor, R.B., 2019. Ponatinib: a novel multi-tyrosine kinase inhibitor against human malignancies. OncoTargets Ther. 12, 635–645. https://doi.org/10.2147/OTT.S189391.

Tang, Z., Yuan, X., Du, R., Cheung, S.H., Zhang, G., Wei, J., Zhao, Y., Feng, Y., Peng, H., Zhang, Y., et al., 2015. BGB-283, a novel RAF kinase and EGFR inhibitor, displays potent antitumor activity in BRAF-mutated colorectal cancers. Mol. Cancer Therapeut. 14, 2187–2197. https://doi.org/10.1158/1535-7163.MCT-15-0262.

Vangone, A., Bonvin, A.M., 2015. Contacts-based prediction of binding affinity in protein-protein complexes. eLife 4, e07454. https://doi.org/10.7554/eLife.07454.

Villanueva, J., Vultur, A., Herlyn, M., 2011. Resistance to BRAF inhibitors: unraveling mechanisms and future treatment options. Cancer Res. 71, 7137–7140. https://doi.org/10.1158/0008-5472.CAN-11-1243.

Wan, P.T., Garnett, M.J., Roe, S.M., Lee, S., Niculescu-Duvaz, D., Good, V.M., Jones, C.M., Marshall, C.J., Springer, C.J., Barford, D., et al., 2004. Mechanism of activation of the RAF-ERK signaling pathway by oncogenic mutations of B-RAF. Cell 116, 855–867. https://doi.org/10.1016/s0092-8674(04)00215-6.

Wang, L., O'Mara, M.L., 2021. Effect of the force field on molecular dynamics simulations of the multidrug efflux protein P-glycoprotein. J. Chem. Theor. Comput. 17, 6491–6508. https://doi.org/10.1021/acs.jctc.1c00414.

Widodo, N., Priyandoko, D., Shah, N., Wadhwa, R., Kaul, S.C., 2010. Selective killing of cancer cells by Ashwagandha leaf extract and its component Withanone involves ROS signaling. PLoS One 5, e13536. https://doi.org/10.1371/journal.pone.0013536.

Wu, J., Omene, C., Karkoszka, J., Bosland, M., Eckard, J., Klein, C.B., Frenkel, K., 2011. Caffeic acid phenethyl ester (CAPE), derived from a honeybee product propolis, exhibits a diversity of anti-tumor effects in pre-clinical models of human breast cancer. Cancer Lett. 308, 43–53. https://doi.org/10.1016/j.canlet.2011.04.012.

Xue, L.C., Rodrigues, J.P., Kastritis, P.L., Bonvin, A.M., Vangone, A., 2016. PRODIGY: a web server for predicting the binding affinity of protein-protein complexes. Bioinformatics 32, 3676–3678. https://doi.org/10.1093/bioinformatics/btw514.

Yadav, D.K., Kumar, S., Saloni, Singh, H., Kim, M.H., Sharma, P., Misra, S., Khan, F., 2017. Molecular docking, QSAR and ADMET studies of withanolide analogs against breast cancer. Drug Des. Dev. Ther. 11, 1859–1870. https://doi.org/10.2147/DDDT.S130601.

Yu, Y., Katiyar, S.P., Sundar, D., Kaul, Z., Miyako, E., Zhang, Z., Kaul, S.C., Reddel, R.R., Wadhwa, R., 2017. Withaferin-A kills cancer cells with and without telomerase: chemical, computational and experimental evidences. Cell Death Dis. 8, e2755. https://doi.org/10.1038/cddis.2017.33.